FISEVIER

Contents lists available at ScienceDirect

Dyes and Pigments

journal homepage: www.elsevier.com/locate/dyepig



Electronic nature of new styryl dye bases: Linear photophysical, photochemical, and transient absorption spectroscopy studies



Ye.O. Shaydyuk^a, O.P. Boyko^a, O.D. Kachkovsky^b, Yu.L. Slominsky^c, J.L. Bricks^c, K.D. Belfield^d, M.V. Bondar^{a,*}

- ^a Institute of Physics, Prospect Nauki, 46, Kyiv-28, 03028, Ukraine
- b V.P. Kukhar Institute of Bioorganic Chemistry and Petrochemistry, Murmanskaya Street, 1, Kyiv, 02660, Ukraine
- ^c Institute of Organic Chemistry, Murmanskaya Street, 5, Kyiv, 02660, Ukraine
- d Department of Chemistry and Environmental Science, College of Science and Liberal Arts, New Jersey Institute of Technology, 323 Martin Luther King, Jr. Boulevard, Newark, NJ, 07102, USA

ARTICLE INFO

Keywords: Styryl dyes Femtosecond transient absorption spectroscopy Twisted intramolecular charge transfer DFT quantum chemical modeling

ABSTRACT

The features of the electronic structures of a series of new styryl dye bases were investigated and characterized by their steady-state and time-resolved spectral properties, including femtosecond transient absorption spepctroscopy and DFT quantum chemical calculations. The steady-state absorption and fluorescence spectra, fluorescence quantum yield, and lifetimes in solvents of different polarity at room temperature revealed specific redistribution of the electronic density and rearrangements in molecular geometry after electronic excitation influenced by the dimethylamino end substituents. Fast relaxation processes in the electronic structures of new styryl dye bases and the nature of their time-resolved excited state absorption spectra were investigated with femtosecond temporal resolution, and the role of twisted intramolecular charge transfer (TICT) effects was shown. Quantum chemical calculations of the electronic structure of the new styryl dye bases were performed using non-empirical Time Dependent Density Functional Theory level, and were in good agreement with experimental data.

1. Introduction

The nature of electronic structures of styryl dye bases and their fast vibronic relaxation processes in the excited state are of considerable scientific interest in a broad range of fundamental and practical research areas, including organic optoelectronics [1-3], ion sensing technologies [4-6], fluorescence microscopy imaging [7,8], amplified spontaneous emission phenomena [9], and fluorescence reporting systems [10]. Linear photophysical properties of specific types of styryl dye bases were reported earlier [4,8,11], and the nature of their excited electronic states and the peculiarities of corresponding dipole transitions were investigated using various experimental techniques in combination with quantum chemical descriptions [12,13]. The effects of substituents in the molecular structures, solvent properties, photoisomerization, and protonation processes on the absorption and fluorescence characteristics of several 2-(4'-R-styryl)-benzoxazoles were shown, and two competitive deactivation pathways of their excited states were elucidated [3].

New styryl dye bases with specific functional groups were

developed in Ref. [10], as a fluorescence probes for monitoring of the microscopic structural changes in sol-gel materials for technological needs. A combination of the efficient intramolecular charge transfer and fast hydrogen bonding processes in the excited state of bisamidopyridine receptor with two styryl base chromophores was proposed in Ref. [4] to substantially increase the anion binding sensitivity. The inversion of the direction of the permanent dipole moment was determined in the excited electronic state of thiastyryls with trifluoromethyl substituents [13], and the nature of their lowest electronic transitions was ascertained.

Nonlinear optical properties and fast relaxations in the ground and excited states of styryl dye bases are scarcely reported in scientific literature [9,11,12], and therefore is a subject of particular interest. The nature of fast relaxation processes in the first excited electronic state of the styryl benzothiazole derivatives was investigated using a femtosecond transient absorption technique [11,12], demonstrating the role of solvation dynamics and twisted intramolecular charge transfer (TICT) effects [14]. The degenerate two-photon absorption (2 PA) spectra of dimethylamino and trifluoromethyl substituents of styryl dye bases

E-mail address: mike_bondar@hotmail.com (M.V. Bondar).

^{*} Corresponding author.

Fig. 1. Chemical structures of styryl dye bases 1-3.

were measured over a broad spectral range by the open aperture Z-scan method [15], with values of 2 PA cross sections up to ~ 100 GM being reported [12].

Here we report a comprehensive investigation of the steady-state and time-resolved spectral properties of new styryl dye bases N,N-dimethyl-4-(2-(naphtho [1,2-d]thiazol-2-yl)vinyl)aniline (1), 2-(4-(tri-fluoromethyl)styryl)naphtho [1,2-d]thiazole (2), and 2-(4-iso-propylstyryl)-N,N-dimethylbenzo [d]thiazol-6-amine (3) (Fig. 1), including their primary photophysical and photochemical parameters obtained in organic solvents at room temperature. The peculiarities of the electronic distribution in the ground and excited states of 1–3, fast relaxation processes, and time-resolved excited state absorption (ESA) spectra were analyzed based on experimental femtosecond transient absorption pump-probe data and quantum chemical calculations performed at the non-empirical time dependent density functional theory (TD-DFT) level.

2. Experimental section

2.1. Synthetic procedure, linear spectroscopic and photochemical measurements

A series of styryl dyes, 1–3, was synthesized by condensation of 2-methylnaphto [1,2-d]thiazole or 2-methyl-6-dimethylaminobenzothiazole with the corresponding 4(R)-substituted benzadehydes in dimethylsulfoxide in the presence of 35% aqueous solution of tetraethylammonium hydroxide or powdered potassium hydroxide at $70\,^{\circ}$ C [11,16–18]. The structures and purity of the new compounds were confirmed by NMR spectroscopy and elemental analysis.

N,N-dimethyl-4-(2-(naphtho [1,2-d] thiazol-2-yl)vinyl)aniline. 4.5 mmol of 2-methylnaphto [1,2-d] thiazole and 5 mmol of 4-dimethylaminobenzaldehyde were heated in 5 ml of DMSO at 70 °C (bath temperature) in the presence of 0.2 ml of 35% tetraethylammonium hydroxide (water solution) for 5 h. After cooling down to room temperature, water (10 ml) was added to the crystallized mass. The resulting precipitate was filtered out, washed with water and dried. Pure product was obtained over the chromatography on silica gel with chloroform as an eluent. Yield – 1.12 g (75%): 1 H NMR (300 MHz, CDCl₃): 5 ppm 8.81 (1H, d, 5 = 8.4 Hz), 7.94 (1H, d, 5 = 7.8 Hz), 7.87 (1H, d, 5 = 8.7 Hz), 7.67 (1H, t, 5 = 6.9 Hz), 7.62–7.45 (4H, m), 7.35 (1H, d, 5 = 15.9 Hz), 6.74 (2H, d, 5 = 9.0 Hz),

3.04 (6H, s). Elemental analysis: calculated for $C_{21}H_{18}N_2S$ (330.44), C 76.32, H 5.49, S 9.70. Found C 76.02, H 5.42, S 9.66.

2-(4-(trifluoromethyl)styryl)naphtho [1,2-d] thiazole. 4.5 mmol of 2-methylnaphto [1,2-d]thiazole and 5 mmol of 4-trifluoromethylbenzaldehyde were heated in 3 ml of DMSO in the presence of 0.2 g of potassium hydroxide powder at 70 °C (bath temperature) for 5 h. After cooling down to room temperature, water (10 ml) was added to the reaction mixture. The precipitate formed was rubbed into powder, filtered out, washed with water and dried. Pure product was chromatographed on silica gel with chloroform as an eluent. Yield – 0.5 g (31%). ¹H NMR (300 MHz, CDCl₃): $\delta_{\rm ppm}$ 8.82 (1H, d, J = 8.1 Hz), 7.95 (1H, d, J = 8.7 Hz), 7.80 (1H, d, J = 8.7 Hz), 7.69 (1H, t, J = 7.3 Hz), 7.65–7.38 (5H, m), 7.12 (1H, d, J = 8.7 Hz), 7.09 (1H, d, J = 8.4 Hz). ¹⁹F (376 MHz, CDCl₃): $\delta_{\rm ppm}$ 63.31 (3F). Elemental analysis: calculated for C₂₀H₁₂F₃NS (355.37), C 67.59, H 3.40, S 9.02. Found C 67.40, H 3.52, S 8.75.

2-(4-isopropylstyryl)-N,N-dimethylbenzo[d] thiazol-6-amine.

2 mmol of 2-methyl-6-dimethylbenzo [d]thiazole and 2.2 mmol of 4-isopropyl benzaldehyde was heated in 3 ml of DMSO at 70 °C (bath temperature) in the presence of 0.2 ml of 35% tetraethylammonium hydroxide (water solution) for 5 h. The reaction mixture was cooled down to room temperature and left overnight. The next day water (10 ml) was added and the resulting precipitate was filtered out, washed with water, dried, and crystallized from toluene. Yield - 0.25 g (39%). $^1\mathrm{H}$ NMR (300 MHz, CDCl₃): δ_{ppm} 7.81 (1H, d, J=9.1 Hz), 7.48 (2H, d, J=8.1 Hz), 7.33 (2H, s), 7.25 (2H, d, J=8.1 Hz), 7.06 (1H, d, J=2.3 Hz), 6.32 (1H, dd, J=9.1, 2.3 Hz), 3.03 (6H, s), 2.93 (1H, m, J=6.8 Hz), 1.27 (6H, d, J=6.8 Hz). Elemental analysis: calculated for $C_{20}H_{22}N_2S$ (322.47), C 74.49, H 6.88, S 9.94. Found C 74.17, H 6.69, S 9.66.

All linear photophysical and photochemical parameters of 1-3 were obtained in spectroscopic grade cyclohexane (CHX) and acetonitrile (ACN) at room temperature. Solvents were purchased from commercial suppliers and used without further purification. The steady-state onephoton absorption (1 PA) spectra were measured with a Shimadzu model 2450 UV-visible spectrophotometer using standard spectrophotometric quartz cuvettes with 1 cm path length and dye concentrations $C \sim 10^{-5} \,\mathrm{M}$. The steady-state fluorescence spectra were obtained using CM 2203 spectrofluorimeter (Solar, Belarus) with 1 cm path length spectrofluorimetric quartz cuvettes and low concentrations, $C \sim 10^{-6}$ M, to avoid reabsorption effects [14]. All fluorescence spectra were corrected on the spectral responsivity of the detection system. The values of the fluorescence quantum yields, Φ_{fl} , were determined by a relative method with 9,10-diphenyl-anthracene in CHX as a standard [14]. The lifetimes of fluorescence emission of 1-3 were measured using a Life Spec-II spectrometer (Edinburgh Instruments Ltd) and standard spectrofluorimetric quartz cuvettes with dilute solutions.

The determination of the photodecomposition quantum yields, Φ_{ph} , of **1–3** was performed by the absorption methodology described previously in detail [19]. Corresponding values of Φ_{ph} can be obtained with the use of the equation [19].

$$\Phi_{ph} = \frac{[D(\lambda, 0) - D(\lambda, t_0)] \cdot N_A}{\varepsilon(\lambda) \cdot 10^3 \cdot \int_{\lambda}^{t_0} \int_0^{t_0} I(\lambda) \cdot [1 - 10^{-D(\lambda, t)}] \cdot d\lambda \cdot dt}$$
(1)

where $D(\lambda, 0)$, $D(\lambda, t_0)$, N_A , λ , $\varepsilon(\lambda)$ and t_0 are the initial and final values of the sample absorbance, Avogadro's number, excitation wavelength (cm), extinction coefficient ($\mathbf{M}^{-1}\cdot\mathbf{cm}^{-1}$), and irradiation time (s), respectively; $I(\lambda)$ is the spectral distribution of the excitation irradiance. The irradiation of the samples was performed using a light emitting diode with $\lambda \approx 400$ nm and average beam irradiance ≈ 40 mW/cm².

2.2. Femtosecond transient absorption pump-probe spectroscopic measurements

Time-resolved ESA spectra and fast intramolecular relaxation

processes in 1-3 were investigated using transient absorption pumpprobe technique with femtosecond excitation, and was described in detail previously [11,20]. Briefly, the exit laser beam of a regenerative amplifier Legend F-1K-HE (laser system from Coherent, Inc.) with wavelength at ≈ 820 nm and 1 kHz repetition rate was split into two channels. The first beam was frequency-doubled with 1 mm BBO crystal to produce second harmonic and used as a pump beam with pulse energy $E_P \leq 20 \,\mu\text{J}$ and pulse duration $\tau_P \approx 140 \,\text{fs}$ (FWHM). It should be mentioned that pump fluence did not exceed $\sim 1 \text{ mJ/cm}^2$. The second part of the splitting laser beam at 820 nm was focused into 3 mm sapphire plate to generate a white light continuum (WLC), that served as a weak probe beam with $E_P \approx 10 \, \text{nJ}$. The spectra of light transmitted through sample solutions were probed with WLC pulses were measured with an Acton SP500i spectrometer and Spec-10 CCD camera (Princeton Instruments, Inc.). An optical delay line M-531. DD (PI, Ltd.) was used to obtain a variable time delay between the pump and probe pulses, and total temporal resolution of the employed technique was estimated as \leq 400 fs. It is worth mentioning that the sample solutions were placed into 1 mm flow cells to avoid thermooptical and photochemical distortions.

2.3. Details of computational analysis

Quantum-chemical calculations were performed to study the dependence of electronic structure-properties relationships of 1–3; the non-conjugated branched alkyl groups were modeled by the simplest methyl (CH₃) groups. The Gaussian 03 package [21] was the software of choice for all calculations. The equilibrium geometry of each dye molecule in the ground state was optimized using the non-empirical DFT/6-31G (d,p)/CAM-B3LYP method. Optimized molecular geometries in the excited electronic state and corresponding parameters of electronic transitions of 1–3 were calculated with the non-empirical TD-DFT/6-31G (d,p)/CAM-B3LYP method. Although this approach has some difficulties for the determination of the absolute absorption maxima [22,23], it is sufficiently accurate to correctly analyze the nature of electron transitions.

3. Results and discussion

3.1. Linear photophysics and photochemical stability of 1-3

The main photophysical and photochemical parameters of new styryl dye bases 1–3, including steady-state 1 PA and corrected fluorescence spectra, fluorescence kinetics, quantum yields, and lifetimes are presented in Table 1 and Figs. 2 and 3. According to these data, all linear absorption spectra of 1–3 exhibited a weak dependence on

solvent polarity and relatively small extinction coefficients in the main long wavelength absorption band, $\varepsilon^{max} \approx (24\text{--}38)\cdot 10^3\,\text{M}^{-1}\text{cm}^{-1}$.

By contrast, compound 2 exhibited relatively small solvatochromism (Fig. 2, b) and the most pronounced vibronic structure. Based on the assumption that the long wavelength 1 PA bands of 1-3 are mainly related to the single electronic transition $S_0 \rightarrow S_1$ (that is typical for similar styryl dye bases [11,12] and confirmed by quantum chemical analysis in sec. 3.3), the values of transition dipoles, μ_{01} , can be calculated as $\mu_{01}^{cal} \approx 0.096 \cdot \sqrt{\int \varepsilon(\nu) \cdot d\nu / \nu^{max}}$ [24] (where frequency $\nu = 1/\lambda_{ab}^{max}$ in cm⁻¹ and extinction coefficient $\varepsilon(\nu)$ in M⁻¹cm⁻¹), with corresponding data presented in Table 1. Accordingly, transition dipoles were in the range of \approx 6-8 D and nicely correlated with the values of ε^{\max} . All observed kinetic curves of the fluorescence emission of 1-3 are characterized by a single-exponential decay (Fig. 3) and obtained lifetimes, τ_{fl} , and fluorescence quantum yields, Φ_{fl} , exhibit weak dependence on solvent polarity (Table 1). It should be mentioned that in contrast to the similarity of the linear absorption properties of 1-3, the values of their Φ_{fl} exhibit large differences depends on the molecular structure with the specific role of dimethylamino end substituents. Nearly the same differences were observed for τ_{fl} , that is indicative of the close values of the corresponding natural radiative lifetimes [14]. The experimental, τ_{fl} , and calculated, τ_{fl}^{cal} (using Strickler-Berg approach [25]), lifetimes of 2 and 3 are in acceptable agreement with each other (see Table 1). Weak discrepancies between τ_{fl} and τ_{fl}^{cal} for **3** can be related to a generally weak electronic transition $S_0 \rightarrow S_1 (\varepsilon^{max} < 3.1 \cdot 10^4 \, \text{M}^{-1} \text{cm}^{-1})$ and specific changes in the strength of vibronic interactions in the excited state [25].

Dramatic decreases in the values of Φ_{fl} and τ_{fl} for 1 in all solvents can be related to the TICT effect in the excited state S_1 [26] resulting from the rotation of the dimethylamino substituent of the aromatic ring along with possible central double bond isomerization. It is interesting to mention that the dimethylamino moiety in the benzothiazole component of 3 didn't lead to a dramatic decrease in the fluorescence efficiency, as was shown previously for similar styryl dye bases [12].

The quantitative investigation of the photochemical stability of 1–3 was performed in air-saturated solutions at room temperature under continuous-wave irradiation in the main 1 PA bands. The values of photodecomposition quantum yields, Φ_{ph} , were determined by the absorption method [19] using equation (1) and corresponding data are presented in Table 1. The styryl dye bases exhibited increase in photostability in more polar solvent (ACN) with the highest level up to 10^{-7} for 1. Photostability of other solutions were 2–3 orders of magnitude smaller, but still comparable with the corresponding parameters of robust laser dyes [27,28], and therefore acceptable for practical applications.

Table 1
The main photophysical and photochemical parameters of 1–3 in CHX and ACN: absorption λ_{ab}^{\max} and fluorescence λ_{fl}^{\max} wavelength maxima, Stokes shifts, maximum extinction coefficients ε^{\max} , calculated transition dipole moments μ_0^{cal} , fluorescence quantum yield Φ_{fl} , experimental τ_{fl} and calculated τ_{fl}^{cal} lifetimes, photodecomposition quantum yield Φ_{ph} , and solvent polarity Δf (orientation polarizability [14]).

Solvent	CHX			ACN		
Compound	1	2	3	1	2	3
$\lambda_{ab}^{\mathrm{max}}$, nm	402 ± 1	375 ± 1	388 ± 1	409 ± 1	369 ± 1	392 ± 1
λ_{fl}^{\max} , nm	468 ± 1	432 ± 1	454 ± 1	524 ± 1	445 ± 1	517 ± 1
Stokes shift, cm ⁻¹ (nm)	3508 (66)	3518 (57)	3747 (66)	5366 (115)	4624 (76)	6168 (125)
$\varepsilon^{\max} \times 10^{-3}$,	30.6 ± 2	24.4 ± 2	30.4 ± 2	37.5 ± 2	28.2 ± 2	29.8 ± 2
M^{-1} ·cm ⁻¹						
μ_{01}^{cal} , D	6.6	5.8	6.9	7.5	6.3	7.1
$\Phi_{fl,~\%}$	1.2 ± 1	14 ± 3	51 ± 3	0.8 ± 0.5	14 ± 3	54 ± 3
τ_{fl} , ns	< 0.13	0.75 ± 0.1	2.04 ± 0.1	< 0.13	0.84 ± 0.1	3.27 ± 0.1
$ au_{\mathrm{fl}}^{\mathrm{cal}}$, ns	-	0.63 ± 0.2	1.6 ± 0.2	-	$0.5~\pm~0.2$	2.3 ± 0.2
Φ_{ph}	$2 \cdot 10^{-5}$	$3.4 \cdot 10^{-4}$	3·10 ⁻⁵	1.10^{-7}	$2.8 \cdot 10^{-4}$	$2 \cdot 10^{-6}$
Δf	0.000248			0.305		

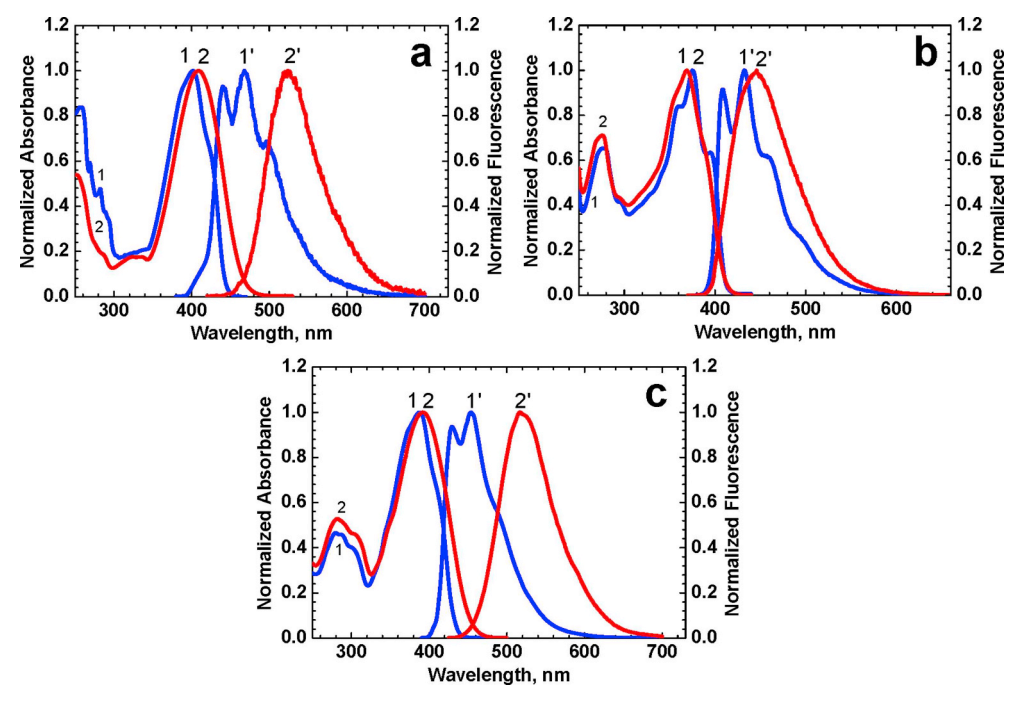


Fig. 2. Normalized steady-state 1 PA (1–2) and fluorescence (1'-2') spectra of 1 (a), 2 (b), and 3 (c) in CHX (1, 1') and ACN (2, 2'). The steady-state fluorescence spectra of 1–3 (Fig. 2, curves 1', 2') exhibited no dependence on excitation wavelength, λ_{ex} (i.e. no violations of the Kasha's rule [14]), and noticeable vibrational structure in nonpolar CHX. Styryl dye bases 1 and 3 were characterized by a relatively large solvatochromic effect, where Stokes shifts increased by a factor of \sim 2 with increase in solvent polarity (see Table 1). This is related to noticeable changes in the stationary dipole moments of these compounds under electronic excitation, and can presumably be assigned to the dominant role of dimethylamino end substituents in the electronic redistribution in the corresponding molecular structures after $S_0 \rightarrow S_1$ transition (S_0 and S_1 are the ground and first excited electronic state, respectively).

3.2. Transient absorption spectroscopy of styryl dye bases 1-3

Fast relaxation processes and time-resolved ESA spectra of the new styryl dyes were investigated in air-saturated ACN at room temperature using femtosecond pump-probe setup [11], and are presented in Fig. 4(a–c) and (d-f), respectively. The kinetic dependences $\Delta D = f(\tau_D)$

(ΔD and τ_D are the induced optical density and time delay between probe and pump pulses, respectfully) reveal population of the first excited state S₁ for 1–3 within the timeframe of \leq 0.8 ps. The positive values of ΔD in the fluorescence spectral range with negligible ground state absorption are indicative of the main role of ESA effects in the observed kinetic dependences. These dependences for compounds 2

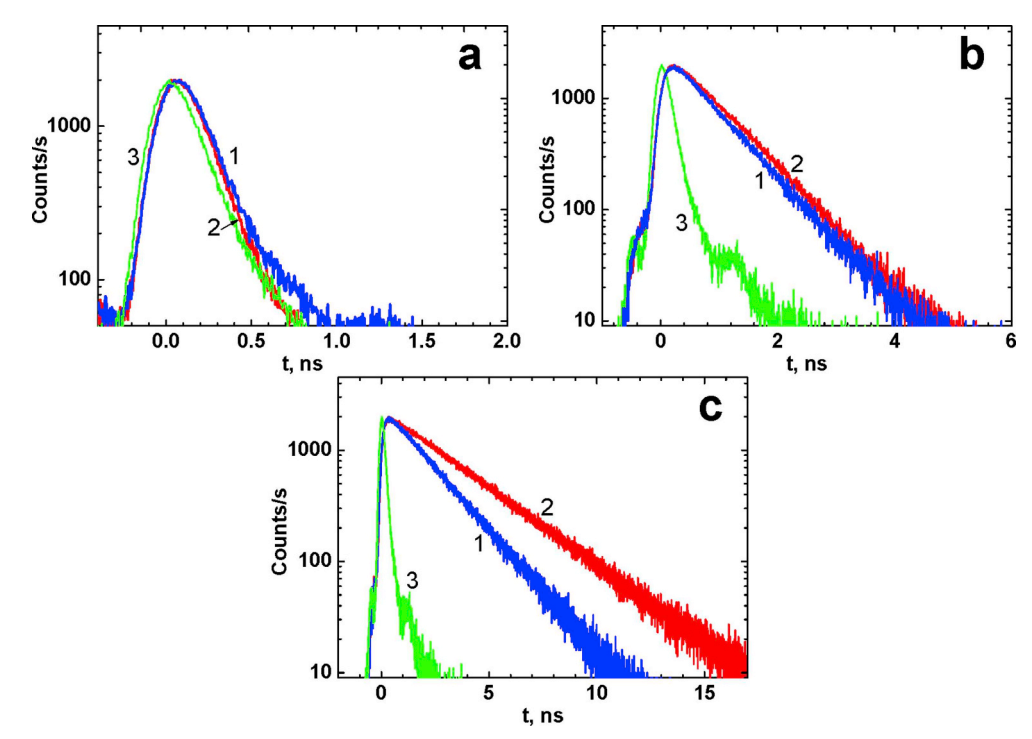


Fig. 3. Fluorescence decay kinetic of 1 (a), 2 (b), and 3 (c) in CHX (1) and ACN (2); instrument response function (3).

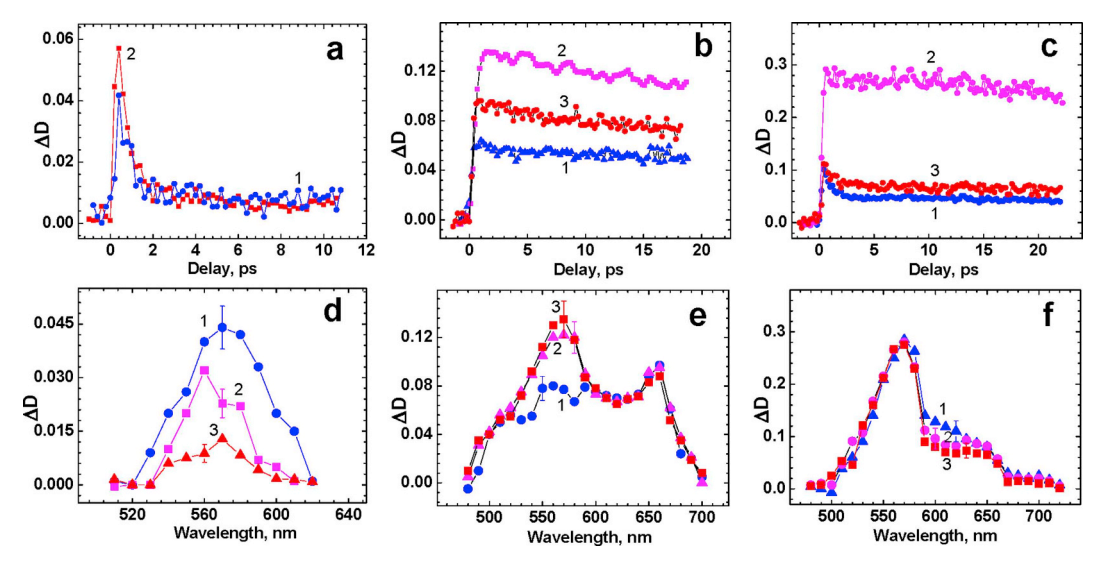


Fig. 4. Transient absorption dependences, $\Delta D = f(\tau_D)$, (a–c) and time-resolved ESA spectra (d–f) of **1** (a, d), **2** (b, e), and **3** (c, f) in ACN. Probe wavelengths: (a) 550 nm (1), 580 nm (2); (b) 510 nm (1), 570 nm (2), and 660 nm (3); (c) 520 nm (1), 570 nm (2), and 620 nm (3); time delay, τ_D , in (d–e): 0.6 ps (1), 1 ps (2), and 5 ps (3).

and 3 exhibit weak evidence of solvate cage reorganization [29,30] and/ or Frank-condon [31] relaxation processes, without any indication of possible TICT effects [32,33]. Induced values of ΔD slowly relaxed to zero in accordance with the corresponding fluorescence lifetimes τ_{fl} . On the other hand, dye 1 exhibited noticeable fast relaxation processes with a characteristic time of $\sim 1-2$ ps that can be attributed to the TICT effect, as was observed previously for styryl dye bases with dimethylamino substituents on the aromatic ring system [12], and is in good agreement with the steady-state spectral data of 1 and its ESA spectra (Fig. 4d). The analysis of the time-resolved ESA spectra of 2 and 3 (Fig. 4e and f) reveals two components in the vibronic relaxation processes, which can be related to different temporal behaviour of several ESA bands that compose the total ESA spectrum of 2 and 3. Corresponding fast component is associated with the band at ≈ 570 nm for 2 and \approx 620 nm for 3. Assumingly, all these peculiarities are an evidence of specific stabilization processes in the excited states due to solvate reorganization phenomena [29,30,34].

3.3. Theoretical analysis of the electronic structures of 1-3

The nature of the spectral properties of the new styryl dye bases was analyzed theoretically using a non-empirical quantum chemical approach at the DFT/6-31G (d,p)/CAM-B3LYP level of theory. The optimized molecular geometries of 1-3 in the ground electronic state S_0 are presented in Fig. 5a. All molecular structures are planar in the S_0 state except for the methyl terminal groups. Styryl dye bases 1-3 are the neutral derivatives of cationic unsymmetrical polymethine dyes (styryl dyes). In contrast to the parent compounds with equalized bond lengths in the linear chromophore, they are characterized by the essential bond length alternation (Fig. 6a). It is worth mentioning, that after electronic excitation in S_1 state all molecular structures remain planar with noticeable changes in the bond lengths alternation (Fig. 6b). Calculated relaxed scan of the potential energy of 1-3 in S_0 and S_1 state along the torsional angles about the corresponding molecular bonds (see Fig. 5b) are shown in Fig. 7.

For convenience, the dye molecules can be divided into three main components taking part in total conjugation: benzothiazole heterocycle (Het), phenyl cycle (Ph), open polymethine chain (-CH = CH-); as an additional conjugated fragment is the dimethylamino group with its lone electron pair including in π -system. Corresponding bonds are indicated in Fig. 5b as "N-Het" "Het-C", "C = C", "C-Ph", "Ph-N". From the data in Fig. 7, one can see that, after $S_0 \rightarrow S_1$ excitation, compound

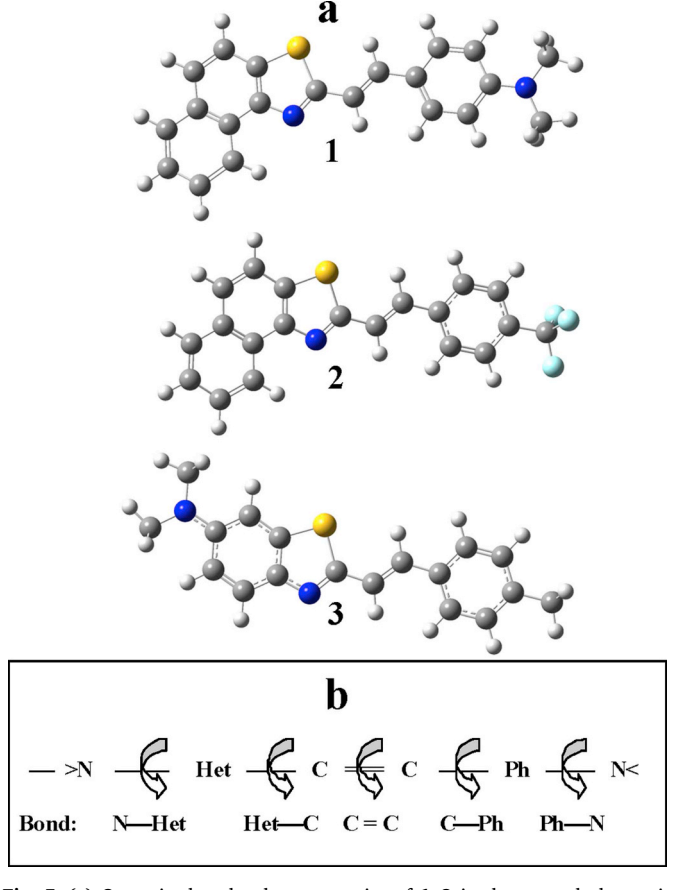


Fig. 5. (a) Optomized molecular geometries of 1-3 in the ground electronic state S_0 . (b) Indications of molecular bonds possible rotations around which were considered in Fig. 7 (see description in the text).

1 can be transformed to more energetically preferable states arising from possible rotations around "C = C" and "C-Ph" bonds (see Fig. 7b and c), in contrast to molecular structure of 2 and 3 (Fig. 7d–i), where no potential minima in twisted conformation can be observed. These data confirm the possibility for 1 to transform into the dark TICT state after electronic excitation $S_0 \rightarrow S_1$, which is in good agreement with the

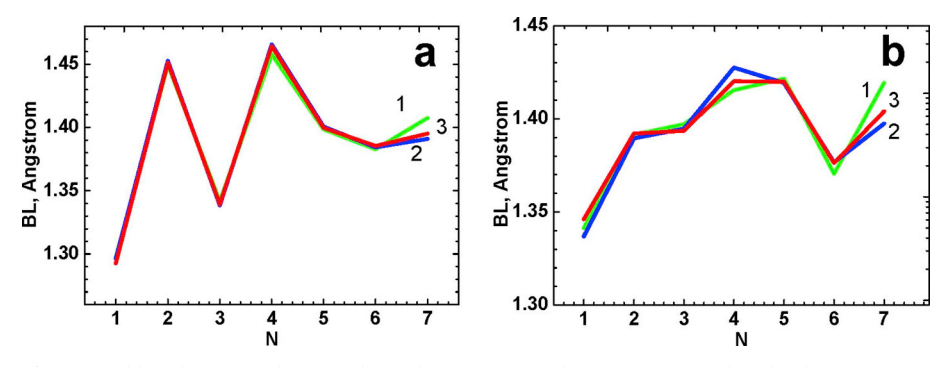


Fig. 6. Bond lengths (BL) in the open chain of 1 (1), 2 (2), and 3 (3) in S_0 (a) and S_1 (b) electronic state.

experimental parameters in Table 1. Calculated characteristics of the main electronic transitions in 1–3 are presented in Table 2. From these data, the first electronic transitions $S_0 \rightarrow S_1$ are determined by "pure" HOMO \rightarrow LUMO configuration for all compounds and the wavelengths of the calculated absorption maxima, λ_{ab}^{cal} , are shifted.

Hypsochromically by 50–60 nm in comparison to the corresponding experimental values, a feature that is typical for non-empirical DFT methods [22,23]. The higher electronic transitions are associated with the nearest molecular orbitals and exhibit noticeably smaller transition dipole moments, in agreement with the weak short wavelengths bands in the experimental absorption spectra.

4. Conclusions

A comprehensive investigation of the steady-state linear photophysical, photochemical, and time-resolved spectral properties of new styryl dyes bases 1–3 was performed in air saturated solutions at room temperature, and were found to be sufficiently photostable. Relatively strong solvatochromic effects in the fluorescence spectra of 1 and 3 was influenced by dimethylamino end substituents in the molecular structures, and no violations of the Kasha's rule were observed for any of the new compounds. The values of fluorescence quantum yields, Φ_{fl} , and lifetimes, τ_{fl} , of 1 were low in all solvents, likely due to TICT in the first excited state S_1 . The possibility of TICT processes in 1 was also confirmed by results from femtosecond transient absorption pump-probe kinetics and quantum chemical modeling based on non-empirical DFT methods. The nature of time-resolved ESA spectra of 1–3 in ACN was analyzed and two components in the vibronic relaxation processes were shown for 2 and 3. The observed traits can be attributed to specific stabilization of the excited states due to solvate reorganization phenomena.

The steady-state and time-resolved spectroscopic data of new styryl

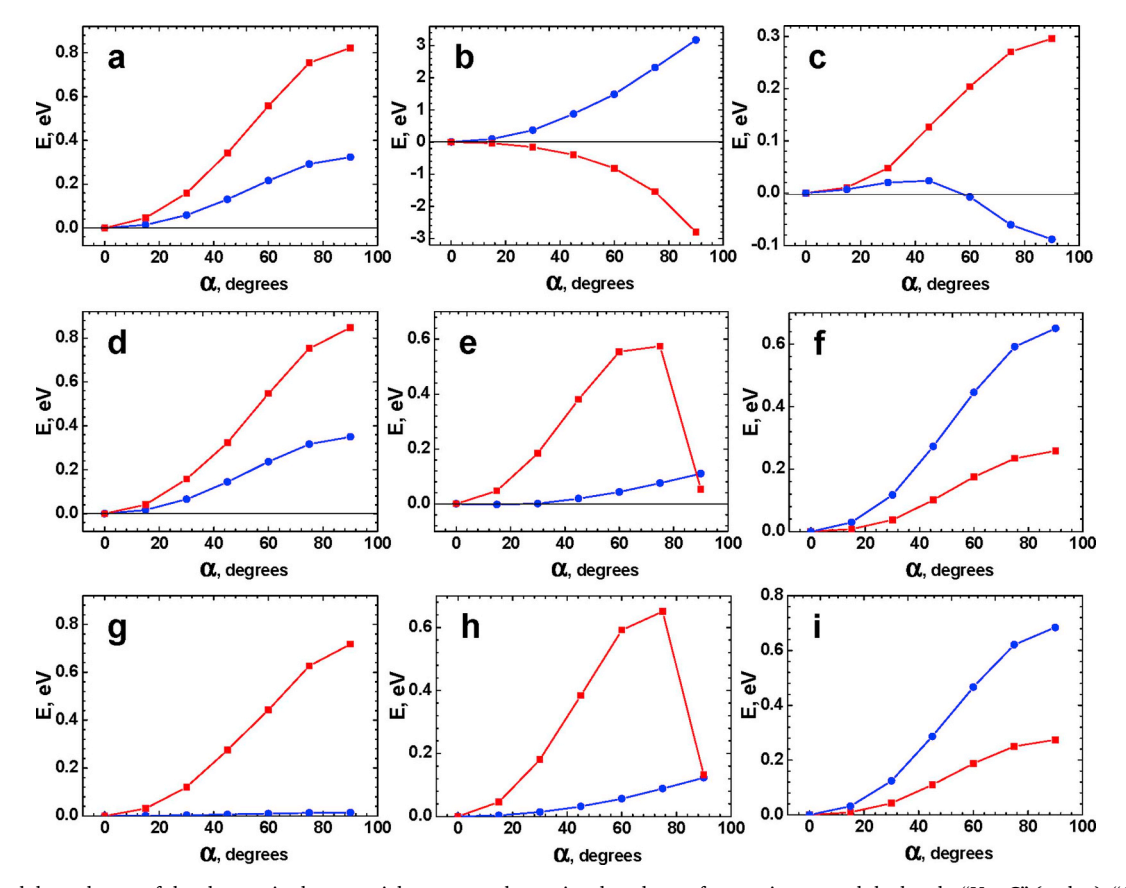


Fig. 7. Calculated dependences of the changes in the potential energy on the torsional angles, α , for rotation around the bonds: "Net-C" (a, d, g), "C = C" (b, e, h), and "C-Ph" (c, f, i) for 1 (a, b, c), 2 (d, e, f), and 3 (g, h, i) in S_0 (blue circles) and S_1 (red squares) electronic state. (For interpretation of the references to colour in this figure legend, the reader is referred to the Web version of this article.)

Table 2 Calculated electronic parameters of 1–3: absorption maxima λ_{ab}^{cal} , oscillator strengths, and orbital configurations (HOMOs and LUMOs represent the highest occupied and lowest unoccupied molecular orbitals, respectively).

Compound	Transition	λ^{cal}_{ab} , nm	Oscillator strength	Main orbital configuration
1	S0 → S1	347	1.3922	0.96 HOMO → LUMO >
	$S0 \rightarrow S2$	290	0.0164	$0.51 \mid \text{HOMO-1} \rightarrow \text{LUMO} >$
				$-0.44 \mid \text{HOMO} \rightarrow \text{LUMO} + 1 >$
	$S0 \rightarrow S3$	276	0.2446	$0.65 \mid \text{HOMO-1} \rightarrow \text{LUMO} >$
				$-0.49 \mid \text{HOMO} \rightarrow \text{LUMO} + 1 >$
2	$S0 \rightarrow S1$	330	0.9138	$0.96 \mid \text{HOMO} \rightarrow \text{LUMO} >$
	$S0 \rightarrow S2$	289	0.1595	$0.75 \mid \text{HOMO-1} \rightarrow \text{LUMO} >$
	$S0 \rightarrow S3$	264	0.6274	$0.75 \mid HOMO \rightarrow LUMO + 1 >$
3	$S0 \rightarrow S1$	336	1.3348	$0.95 \mid \text{HOMO} \rightarrow \text{LUMO} >$
	$S0 \rightarrow S2$	275	0.0041	$0.58 \mid \text{HOMO-1} \rightarrow \text{LUMO} >$
				- 0.57 HOMO → LUMO + 1 >
	$S0 \rightarrow S3$	258	0.0853	$0.74 \mid \text{HOMO-1} \rightarrow \text{LUMO} >$
				$-0.49 \mid \text{HOMO} \rightarrow \text{LUMO} + 1 >$

dye bases suggest potential in the development of new materials with dark TICT states for uses such as stochastic-based superresolution imaging.

Acknowledgements

The authors thank the employees of the NASU Center for collective use of "Laser femtosecond complex" at the Institute of Physics NAS Ukraine. This work is supported by the National Academy of Sciences of Ukraine (grant V/180, VC/188, and VC/201). KDB wishes to acknowledge support from the National Science Foundation (CBET-1517273 and CHE-1726345).

References

- Egbe DAM, Tekin E, Birckner E, Pivrikas A, Sariciftci NS, Schubert US. Effect of styryl side groups on the photophysical properties and hole mobility of PPE-PPV systems. Macromolecules 2007;40:7786–94.
- [2] Kakuta A, Mori Y, Morishita H. The ionization potential of carrier transport materials in relation to the photosensitivity of double layered photoreceptors. IEEE Trans Ind Appl 1981;1A-22(4):383–6.
- [3] Fayed TA, Etaiw SH, Khatab HM. Excited state properties and acid-base equilibria of trans-2-styrylbenzoxazoles. J Photochem Photobiol, A 2005;170:97–103.
- [4] Kovalchuk A, Bricks JL, Reck G, Rurack K, Schulz B, Szumna A, Weißhoff H. A charge transfer-type fluorescent molecular sensor that "lights up" in the visible upon hydrogen bond-assisted complexation of anions. Chem Commun 2004:1946–7.
- [5] Bricks JL, Slominskii JL, Kudinova MA, Tolmachev AI, Rurack K, Resch-Genger U, Rettig W. Syntheses and photophysical properties of a series of cation-sensitive polymethine and styryl dyes. J Photochem Photobiol, A 2000;132:193–208.
- [6] Rettig W, Rurack K, Sczepan M. From cyanine to styryl bases E photophysical properties, photochemical mechanisms, and cation densing abilities of charged and neutral polymethinic dyes. In: Valeor B, Bredas J-L, editors. New trends in fluorescence spectroscopy: applications to chemical and Life Sciences. Berlin: Springer; 2001. p. 125–55.
- [7] Steinmeyer J, Ronicke F, Schepers U, Wagenknecht H-A. Synthesis of wavelengthshifting fluorescent DNA and RNA with two photostable cyanine–styryl dyes as the base surrogate pair. ChemistryOpen 2017;6:514–8.
- [8] Li Q, Jaeki Min J, Ahn Y-H, Namm J, Kim EM, Lui R, Kim HY, Ji Y, Wu H, Wisniewski T, Chang Y-T. Styryl-based compounds as potential in vivo imaging agents for B-amyloid plaques. Chembiochem 2007;8:1679–87.
- [9] Vembris A, Muzikante I, Karpicz R, Sliauzys G, Miasojedovas A, Jursenas S, Gulbinas V. Fluorescence and amplified spontaneous emission of glass forming compounds containing styryl-4h-pyran-4-ylidene fragment. J Lumin 2012;132:2421-6.
- [10] Unger B, Rurack K, Muller R, Jancke H, Resch-Genger U. Microscopic vs. Macroscopic structural evolution of SiO₂ sols and gels employing a tailor-made fluorescent reporter dye. J Mater Chem 2005;15:3069–83.
- [11] Bashmakova NV, Shaydyuk YO, Levchenko SM, Masunov AE, Przhonska OV, Bricks JL, Kachkovsky OD, Slominsky YL, Piryatinski YP, Belfield KD, Bondar MV. Design and electronic structure of new styryl dye bases: steady-state and time-resolved spectroscopic studies. J Phys Chem A 2014;118:4502–9.
- [12] Shaydyuk YO, Levchenko SM, Kurhuzenkau SA, Anderson D, Masunov AE, Kachkovsky OD, Slominsky YL, Bricks JL, Belfield KD, Bondar MV. Linear photophysics, two-photon absorption and femtosecond transient absorption spectroscopy of styryl dye bases. J Lumin 2017;183:360–7.
- [13] Navozenko OM, Naumenko AP, Yashchuk VM, Bricks JL, Slominskii YL, Ryabitskii AB, Kachkovsky OD. Nature of the lowest electron transitions in styryl bases benzothiazole derivatives and analogues bearing para-methoxy and -trifluoromethyl

- substituents in phenylyne moiety. J Mol Struct 2016;1113:32-41.
- [14] Lakowicz JR. Principles of fluorescence spectroscopy. New York: Kluwer; 1999.
- [15] Sheik-Bahae M, Said AA, Wei TH, Hagan DJ, Van Stryland EW. Sensitive measurement of optical nonlinearities using a single beam. IEEE J Quantum Electron 1990;26(4):760–9.
- [16] Dryanska V, Ivanov K. A-hydroxybenzylation and benzylidenation of the methyl group in 2-methyl-1,3-benzoxazole and 2-methyl-1,3-benzothiazole. Synthesis 1976(1):37–8.
- [17] Rurack K, Resch-Genger U, Rettig W. Unusually high cation-induced fluorescence enhancement of a structurally simple intrinsic fluoroionophore with a donor-acceptor-donor constitution. Chem Commun 2000;5:407–8.
- [18] Rurack K, Koval'chuck A, Bricks JL, Slominskii JL. A simple bifunctional fluoroionophore signaling different metal ions either independently or cooperatively. J Am Chem Soc 2001;123(25):6205–6.
- [19] Corredor CC, Belfield KD, Bondar MV, Przhonska OV, Yao S. One- and two-photon photochemical stability of linear and branched fluorene derivatives. J Photochem Photobiol, A 2006;184(1–2):105–12.
- [20] Belfield KD, Bondar MV, Haniff HS, Mikhailov IA, Luchita G, Przhonska OV. Superfluorescent squaraine with efficient two-photon absorption and high photostability. ChemPhysChem 2013;14:3532–42.
- [21] Frisch MJ, Trucks GW, Schlegel HB, Scuseria GE, Robb MA, Cheeseman JR, Montgomery JJA, Vreven T, Kudin KN, Burant JC, Millam JM, Iyengar SS, Tomasi J, Barone V, Mennucci B, Cossi M, Scalmani G, Rega N, Petersson GA, Nakatsuji H, Hada M, Ehara M, Toyota K, Fukuda R, Hasegawa J, Ishida M, Nakajima T, Honda Y, Kitao O, Nakai H, Klene M, Li X, Knox JE, Hratchian HP, Cross JB, Adamo C, Jaramillo J, Gomperts R, Stratmann RE, Yazyev O, Austin AJ, Cammi R, Pomelli C, Ochterski JW, Ayala PY, Morokuma K, Voth GA, Salvador P, Dannenberg JJ, Zakrzewski VG, Dapprich S, Daniels AD, Strain MC, Farkas O, Malich DK, Rabuck AD, Raghavachari K, Foresman JB, Ortiz JV, Cui Q, Baboul AG, Clifford S, Cioslowski J, Stefanov BB, Liu G, Liashenko A, Piskorz P, Komaromi I, Martin RL, Fox DJ, Keith T, Al-Laham MA, Peng CY, Nanayakkara A, Challacombe M, Gill PMW, Johnson B, Chen W, Wong MW, Gonzalez C, Pople JA. Gaussian 03, revision A.1. Pittsburgh, PA: Gaussian, Inc.; 2003.
- [22] Fabian J. TDDFT-calculations of vis/NIR absorbing compounds. Dyes Pigments 2010;84:36–53.
- [23] Jacquemin D, Zhao Y, Valero R, Adamo C, Ciofini I, Truhlar DG. Verdict: time-dependent density functional theory "not guilty" of large errors for cyanines. J Chem Theory Comput 2012;8:1255–9.
- [24] Hales JM, Matichak J, Barlow S, Ohira S, Yesudas K, Brédas J-L, Perry JW, Marder SR. Design of polymethine dyes with large third-order optical nonlinearities and loss Figures of merit. Science 2010;327:1485–8.
- [25] Strickler SJ, Berg RA. Relationship between absorption intensity and fluorescence lifetime of molecules. J Chem Phys 1962;3(4):814–22.
- [26] Chen K-F, Chang C-W, Lin J-L, Hsu Y-C, Yeh M-CP, Hsu C-P, Sun S-S. Photophysical studies of dipolar organic dyes that feature a 1,3-cyclohexadiene conjugated linkage: the implication of a twisted intramolecular charge-transfer state on the efficiency of dye sensitized solar cells. Chem Eur J 2010;16:12873–82.
- [27] Azim SA, Al-Hazmy SM, Ebeid EM, El-Daly SA. A new coumarin laser dye 3-(ben-zothiazol-2-yl)-7-hydroxycoumarin. Optic Laser Technol 2005;37:245–9.
- [28] El-Daly SA, El-Azim SA, Elmekawey FM, Elbaradei BY, Shama SA, Asiri AM. Photophysical parameters, excitation energy transfer, and photoreactivity of 1,4-bis (5-phenyl-2-Oxazolyl)Benzene (POPOP) laser dye. Int J Photoenergy 2012;2012. 458126/1-45812610.
- [29] Kumar KS, Selvaraju C, Padma Malar EJ, Natarajan P. Existence of a new emitting singlet state of proflavine: femtosecond dynamics of the excited state processes and quantum chemical studies in different solvents. J Phys Chem A 2012;116:37–45.
- [30] Liu T, Bondar MV, Belfield KD, Anderson D, Masunov AE, Hagan DJ, Van Stryland EW. Linear photophysics and femtosecond nonlinear spectroscopy of a star-shaped squaraine derivative with efficient two-photon absorption. J Phys Chem C 2016;120:11099–110.
- [31] Wang Y, Liu W, Tang L, Oscar B, Han F, Fang C. Early time excited-state structural evolution of pyranine in methanol revealed by femtosecond stimulated Raman spectroscopy. J Phys Chem A 2013;117:6024–42.

- [32] Nibbering ETJ, Fidder H, Pines E. Ultrafast chemistry: using time-resolved vibrational spectroscopy for interrogation of structural dynamics. Annu Rev Phys Chem 2005;56:337–67.
- [33] Letrun R, Koch M, Dekhtyar ML, Kurdyukov VV, Tolmachev AI, Rettig W, Vauthey E. Ultrafast excited-state dynamics of donor-acceptor biaryls: comparison between
- pyridinium and pyrylium phenolates. J Phys Chem A 2013;117:13112–26.
 [34] Horng ML, Gardecki JA, Papazyan A, Maroncelli M. Subpicosecond measurements of polar solvation dynamics: coumarin 153 revisited. J Phys Chem 1995;99:17311–37.